Quantum resonances due to classical stability islands

P. Gerwinski
Fachbereich Physik, Universität-Gesamthochschule-Essen, 45117 Essen, Germany

P. Šeba
Nuclear Research Institute, 250 68 Řež near Prague, Czech Republic
(Received 4 May 1994)

We have studied the scattering of a one-dimensional particle by a time-periodically kicked potential. In the classical case, this system displays irregular scattering. We show that the presence of a large stability island in the classical phase space leads to sharp resonances in the quantum case. Using the corresponding time-independent system the localization of the resonances is predicted by a first-order perturbation theory. We show that the observed resonance patterns are closely connected with the quantum tunneling between the chaotic and stability regions of the classical phase space.

PACS number(s): 05.45.+b, 47.52.+j, 95.10.Fh

I. INTRODUCTION

Classical irregular scattering has been a subject of vivid interest for more then one decade [1–3]. As a typical example of a transient chaos it recently attracted considerable interest and is a frontier of research on classical chaotic Hamilton systems. Quantum consequences of classical irregular scattering have first been studied by Blümel and Smilansky [4]. They demonstrated that the existence of a classical chaotic repeller implies Ericson fluctuations of the corresponding quantum S matrix.

Meanwhile classical and quantum irregular scattering has been investigated in several models (see, for example Refs. [5,6]). Their common feature was that the classical chaotic repeller (which is responsible for the appearance of the fractally organized singularities in the classical scattering) was fully hyperbolic. This means that the probability density $P(t)$ for a classical particle to stay in the interaction region for a time longer than t is given by [7]

$$P(t) \sim e^{-\alpha t}, \tag{1}$$

where α is connected with the Lyapunov exponent of the repeller and with the corresponding Kol'mogorov-Sinai entropy [8]. In the classical case it implies a self-similar structure of the scattering singularities (a kind of Cantor set). In the quantum case, (1) leads to the absence of long-lived resonances and consequently to Ericson fluctuations of the quantum cross section [4].

In the present paper we will construct a one-dimensional and periodically driven model in which (1) is violated. Depending on the parameters of the model, the corresponding repeller will display a large stability island leading to an algebraic decay of $P(t)$ [9–12]

$$P(t) \sim t^{-\alpha}. \tag{2}$$

The influence of the elliptic domain on the fractal set of the classical scattering singularities will be investigated in Sec. II. The quantum case is discussed in Sec. III, where we show that the existence of a classical island of stability leads to the appearance of sharp resonances. In Sec. IV we will study the mechanism responsible for the resonant behavior: "tunneling" between the regular and the chaotic region in phase space.

II. CLASSICAL DESCRIPTION OF THE MODEL

We study a time-periodically "kicked" scattering system which has the following Hamilton function:

$$H(p,x,t) = \tfrac{1}{2}p^2 + \lambda V(x) \sum_{n=-\infty}^{\infty} \delta(t-n) \tag{3}$$

with the attractive short-range potential $V(x)$

$$V(x) = -\frac{1}{\cosh^2 x}. \tag{4}$$

"Far away" from the scattering center we can neglect the potential and consider the particle as free. Therefore we can fix the asymptotic momentum for $t \to \pm\infty$ for an incoming or outgoing particle as

$$\lim_{t\to-\infty} |p(t) - p_{\text{in}}| = 0, \tag{5}$$

$$\lim_{t\to+\infty} |p(t) - p_{\text{out}}| = 0. \tag{6}$$

The time development of a particle with initial conditions (x_0, p_0) is given by the following stroboscopic map:

$$\begin{aligned} p_{n+1} &= p_n - \lambda V'(x_n), \\ x_{n+1} &= x_n + p_{n+1}. \end{aligned} \tag{7}$$

This map allows us to study the classical properties of the system numerically. When we apply it to a set of ran-

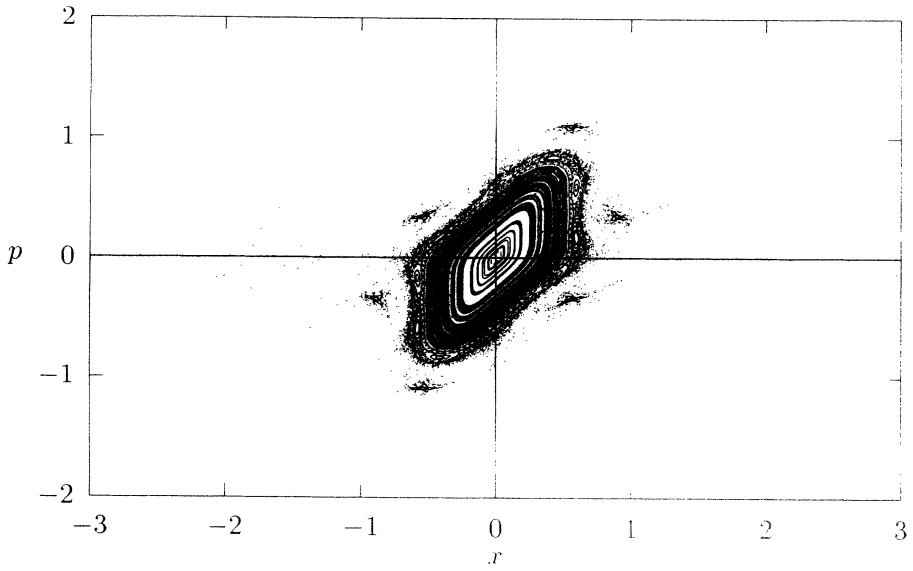

FIG. 1. Poincaré plot for $\lambda = 1$. In the center we see a large "stability island" which is embedded in a chaotic layer.

dom initial conditions, we can plot a Poincaré scenario which shows the structure of the phase space. There are two typical cases: For $\lambda < 2$ we have an elliptic fixed point in the center surrounded by unbroken Kol'mogorov-Arnol'd-Moser tori. We call this region the "stability island" (see Fig. 1); it is embedded in a chaotic layer. For $\lambda > 2$ the fixed point becomes hyperbolic, the stability island disappears and phase space is dominated by chaos (see Fig. 2).

Now we want to compute the delay time of a scattered particle and compare it with formulas (1) and (2). In order to do it, we introduce asymptotic incoming and outgoing coordinates and times by

$$x_{\text{in}} = \lim_{t \to -\infty} x(t) - t p_{\text{in}}, \tag{8}$$

$$x_{\text{out}} = \lim_{t \to +\infty} x(t) - t p_{\text{out}}, \tag{9}$$

$$t_{\text{in}} := -\frac{x_{\text{in}}}{p_{\text{in}}}, \tag{10}$$

$$t_{\text{out}} := -\frac{x_{\text{out}}}{p_{\text{out}}}. \tag{11}$$

Now we are able to define the delay Δt, i.e., the time, the particle spends in the interaction region as

$$\Delta t := t_{\text{out}} - t_{\text{in}}. \tag{12}$$

Using (12), we computed the number of particles with a fixed initial energy E the delay time Δt of which is bigger than a given value t. As predicted in [8], we find a clear exponential decay for the hyperbolic case (see Fig. 3). In presence of a stability island we obtain an algebraic decay (see Fig. 4).

III. QUANTUM MECHANICAL DESCRIPTION

A quantum analog of the map (7) is given by the evolution operator over one period, the Floquet operator. In

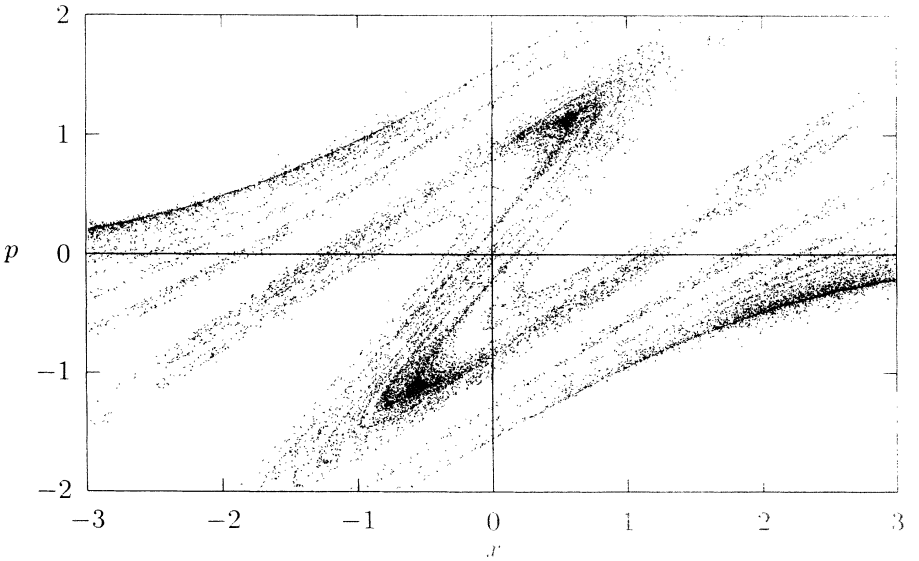

FIG. 2. Poincaré plot for $\lambda = 3$. The phase space is dominated by chaos.

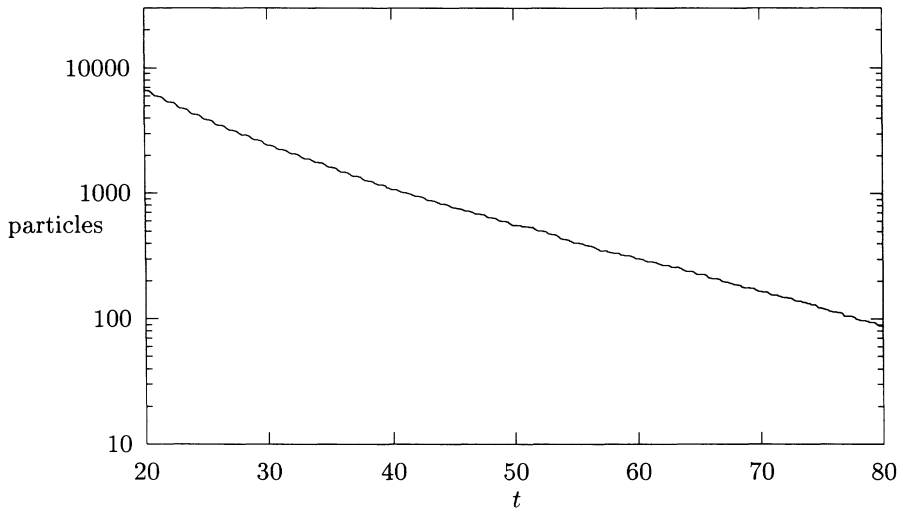

FIG. 3. Number of particles (out of 1 000 000) with a delay time Δt bigger than t for $\lambda = 3$. As expected for the completely chaotic case, it decays exponentially with t.

the present model the Floquet operator has a particularly simple form:

$$F = e^{-\frac{i}{2\hbar}p^2} e^{-\frac{i}{\hbar}\lambda V(x)}. \tag{13}$$

The operator F describes the time evolution of the system: Starting with an initial state $|\psi_0\rangle$ at time $t = 0$ and following its time evolution we get after the nth kick:

$$|\psi_n\rangle = F^n|\psi_0\rangle. \tag{14}$$

In numerical calculations, we evaluate $e^{-\frac{i}{2\hbar}p^2}$ in the momentum representation and $e^{-\frac{i}{\hbar}\lambda V(x)}$ in the position representation. Thus the main part of the calculation time is used for Fourier transforms between both these representations.

We are interested in the properties of the S matrix in dependence on the coupling constant λ. In order to define the quantum S matrix, we use the method of Yajima [13] and Howland [14]. Introducing the Møller operators

$$\Omega_{\pm} = \lim_{n \to \mp\infty} F_0^{-n} F^n P, \tag{15}$$

where F_0 is the free Floquet operator $e^{-\frac{i}{2\hbar}p^2}$ and P is the projector into the absolutely continuous subspace $\mathcal{H}_a$ of F we define the S matrix in the standard way:

$$S = \Omega_-^{\dagger} \Omega_+. \tag{16}$$

S is unitary on $\mathcal{H}_a$ and commutes with the free Floquet operator F_0:

$$[S, F_0] = 0. \tag{17}$$

Consequently the free quasienergy (i.e., the eigenvalue of the free Floquet operator F_0) is conserved during the scattering process.

To construct a basis in which S has a suitable form we start with the eigenfunction $|E, \pm\rangle$ of the free Hamiltonian H_0:

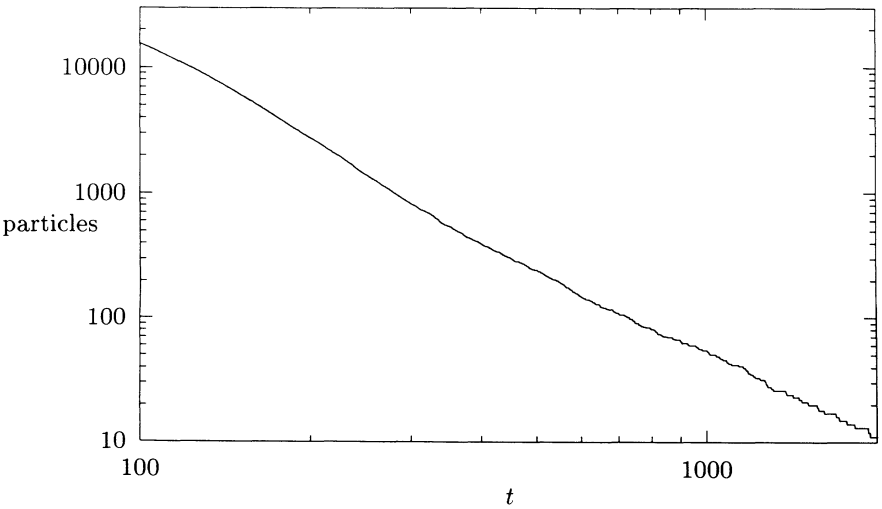

FIG. 4. The same as in Fig. 3, but for $\lambda = 1$. Since we have a stability island, the decay is algebraic.

$$H_0 = -\tfrac{1}{2}\hbar^2 \tfrac{\partial^2}{\partial x^2}, \tag{18}$$

$$H_0|E,\pm\rangle = E|E,\pm\rangle, \tag{19}$$

for positive E.

The eigenvalues of H_0 are two-times degenerate. So $|E,+\rangle$ denotes the eigenstate of H_0 which has energy E and describes a particle traveling from left to right. Similarly $|E,-\rangle$ describes a particle with energy E moving from right to left. In order to obtain the eigenvalues and eigenvectors of the free Floquet operator F_0 we have to compart E with respect to $2\pi\hbar$:

$$\begin{aligned} E &= \Theta + 2\pi\hbar n, \\ & n = 0, \pm 1, \pm 2, \ldots, \\ & 0 \le \Theta < 2\pi\hbar. \end{aligned} \tag{20}$$

Then Θ is the infinitely degenerate eigenvalue of F_0:

$$F_0|E,\pm\rangle = e^{i\Theta}|E,\pm\rangle. \tag{21}$$

Taking into account the degeneracy of the eigenvalue Θ we will denote the corresponding eigenvector as $|\Theta,n,\pm\rangle$

$$|\Theta,n,\pm\rangle = |E,\pm\rangle, \tag{22}$$

where E, n and Θ are connected by (20). For $|\Theta,n,\pm\rangle$ holds

$$\langle\Theta',n',\pm|\Theta,n,\pm\rangle = \delta(\Theta-\Theta')\,\delta_{n,n'}\,\delta_{\pm,\pm}. \tag{23}$$

In such a way $|\Theta,n,\pm\rangle$ is a suitable basis in which the S matrix can be written as

$$\langle\Theta,n,\pm|S|\Theta',n',\mp\rangle = S^{\pm,\mp}_{n,n'}(\Theta)\,\delta(\Theta-\Theta'). \tag{24}$$

$S^{+-}_{n,n'}(\Theta)$ is nothing but the quantum transmission coefficient for a particle coming from the right with initial energy $E_{\text{in}} = \Theta + 2\pi\hbar n$ and moving after the scattering process to the left with energy $E_{\text{out}} = \Theta + 2\pi\hbar n'$. Similarly $S^{-+}_{n,n'}(\Theta)$ describes the same process in the other direction. $S^{++}_{n,n'}(\Theta)$ is the reflection coefficient for the left-moving particle and so on.

The symmetry of the potential $V(x)$ implies

$$\begin{aligned} S^{+-}_{n,n'}(\Theta) &= S^{-+}_{n,n'}(\Theta), \\ S^{++}_{n,n'}(\Theta) &= S^{--}_{n,n'}(\Theta). \end{aligned} \tag{25}$$

Hence, we can simplify the notation and denote

$$\begin{aligned} S^{-}_{n,n'}(\Theta) &:= S^{++}_{n,n'}(\Theta) = S^{--}_{n,n'}(\Theta), \\ S^{+}_{n,n'}(\Theta) &:= S^{+-}_{n,n'}(\Theta) = S^{-+}_{n,n'}(\Theta). \end{aligned} \tag{26}$$

We will call n the *channel number*.

The numerical calculations of $S^{-}_{n,n'}(\Theta)$ for $n = n' = 0$ are presented in Figs. 5–8. In the fully chaotic case with $\lambda = 3$ (Fig. 5) we get Ericson fluctuations as predicted by Blümel and Smilansky [4]. The Θ-autocorrelation function $C^{\pm}_{nn'} := \langle S^{\pm *}_{nn'}(\Theta')S^{\pm}_{nn'}(\Theta'+\Theta)\rangle_{\Theta'}$ (see Fig. 6) is the predicted Lorentzian $|C^{\pm}_{nn'}|^2 = \alpha/(\alpha + (\Theta/\hbar)^2)$ with α as in Eq. (1).

For $\lambda = 1$, where we have a large stability island in the phase space, we get a series of sharp resonances (Fig. 7). As we show next, these resonances are connected with the quantum tunneling into the stability island.

Generally, a time-periodic Hamiltonian (with period 1) can be written as

$$H = \tfrac{1}{2}\hbar^2 \tfrac{\partial^2}{\partial x^2} + \lambda V(x) \sum_{n=-\infty}^{\infty} a_n e^{-i2\pi nt} \tag{27}$$

(in our case all coefficients $a_n = 1$). We can find solutions of the corresponding Schrödinger equation starting with

$$\psi(x,t) = \sum_{n=-\infty}^{\infty} u_n(x) e^{-i2\pi nt} e^{-\frac{i}{\hbar}\Theta t}. \tag{28}$$

Solutions of this type have a sharp free quasienergy Θ. Inserting (28) into the Schrödinger equation we obtain

$$\begin{aligned} u_n''(x) &= 2(\Theta + n2\pi\hbar)u_n(x) \\ &\quad -2\lambda V(x) \sum_{l=-\infty}^{\infty} u_l(x) a_{n-l}, \end{aligned} \tag{29}$$

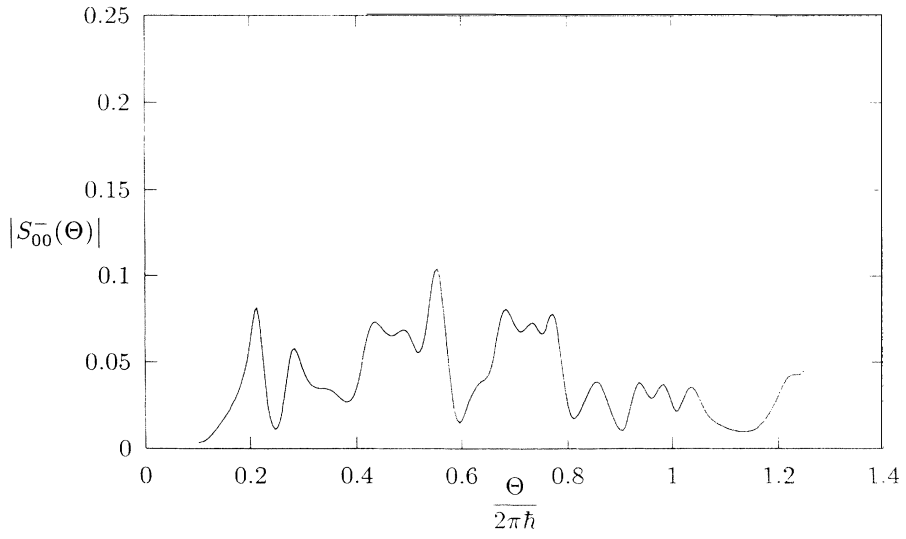

FIG. 5. The reflection coefficient $S^{-}_{00}(\Theta)$ as a function of Θ for the fully chaotic case with $\lambda = 3$ shows Ericson fluctuations as predicted by Blümel and Smilansky [4] ($\hbar = 0.05$).

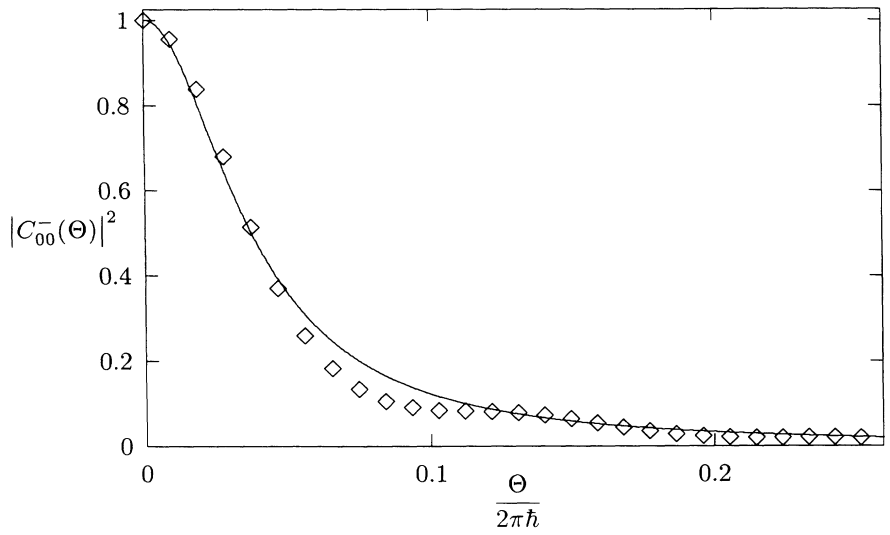

FIG. 6. The Θ-autocorrelation function $|C_{00}^{-}|^2$ for $S_{00}^{-}(\Theta)$. The solid line shows the Lorentzian $\alpha/[\alpha + (\Theta/\hbar)^2]$ predicted by Blümel and Smilansky [4] with α being the classical decay rate as in Eq. (1). The numerical value $\alpha = 0.055$ is taken from the slope of a fitted line in Fig. 3.

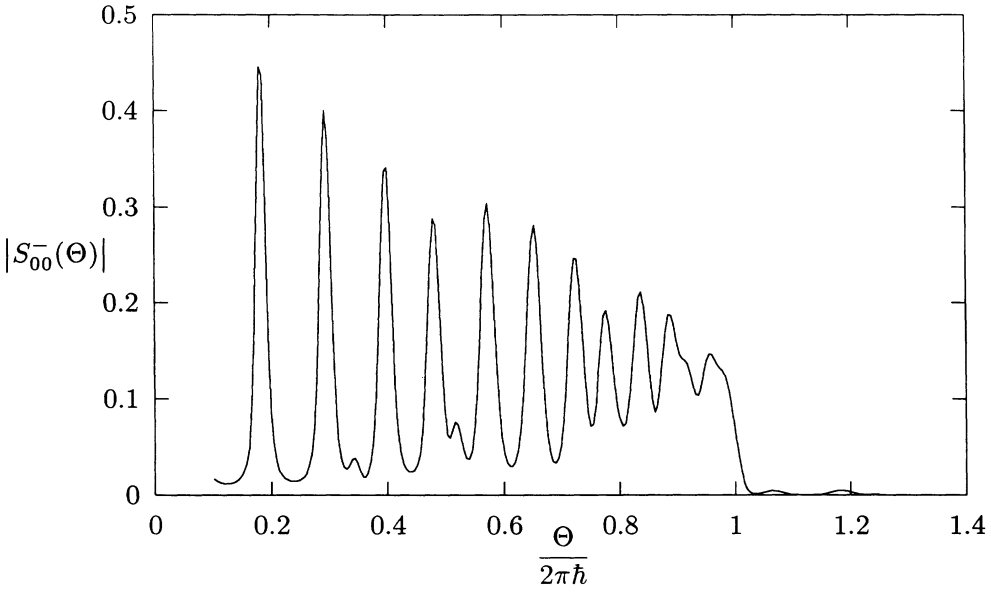

FIG. 7. The reflection coefficient $S_{00}^{-}(\Theta)$ as a function of Θ in the presence of a large stability island for $\lambda = 1$ displays a sequence of sharp maxima ($\hbar = 0.05$).

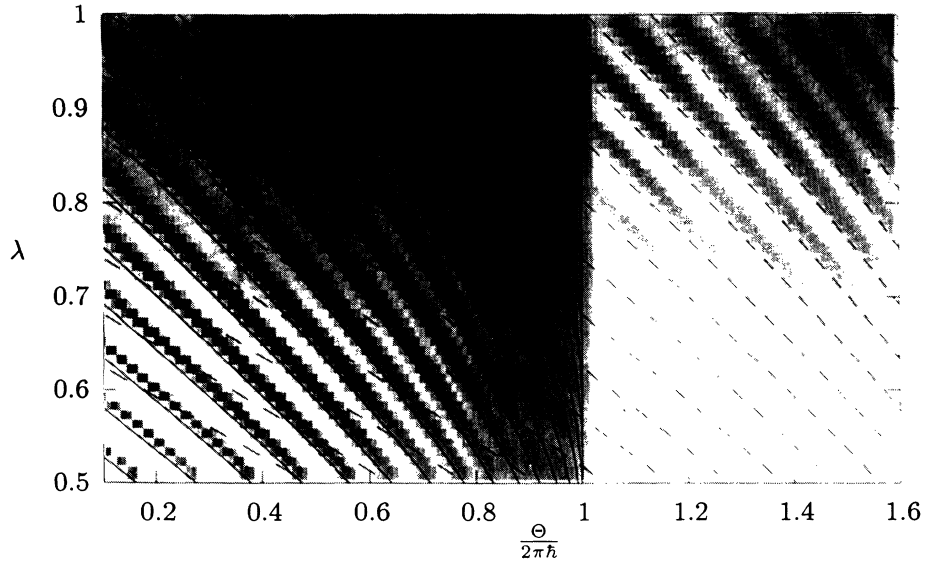

FIG. 8. Gray scale plot of the total reflection coefficient $S^{-}(\Theta)$ as a function of Θ and λ. The solid lines stand for eigenvalues E_k of a corresponding time-independent system, shifted by $2\pi\hbar$; the dashed lines denote $E_k + 2 \times 2\pi\hbar$.

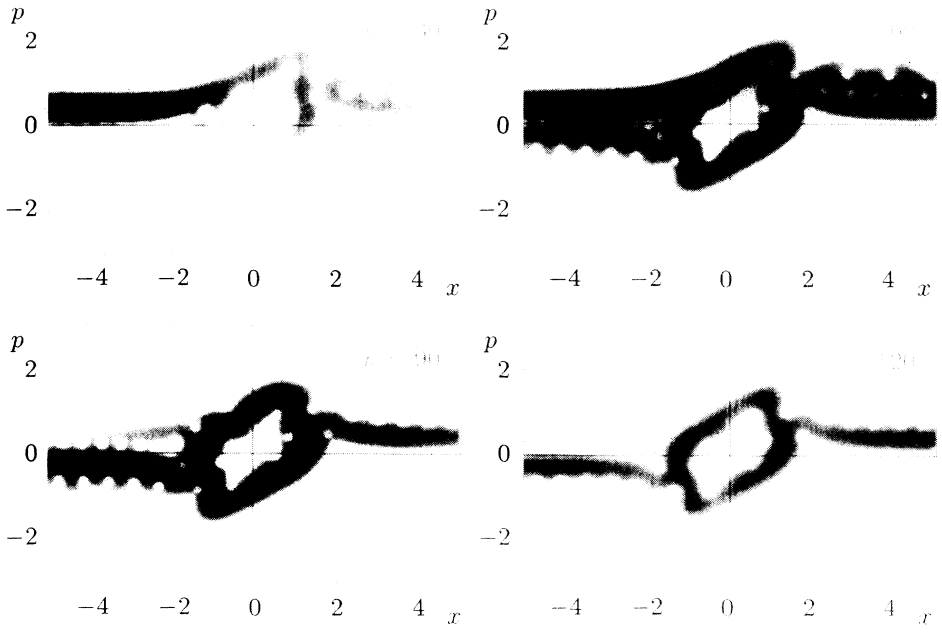

FIG. 9. The Husimi function of a scattered quantum particle with maximum reflection coefficient. The wave function enters a quasistable orbit at the border of the classical stability island.

for each n. The "diagonal" part $l = n$ of this equation describes a time-independent dynamic:

$$u_n''(x) = 2(\Theta + n2\pi\hbar)u_n(x) - 2\lambda V(x)u_n(x)a_0. \quad (30)$$

In our case with $a_0 = 1$ and $V(x) = -1/\cosh^2 x$ we can find the eigenvalues of this equation analytically. For $\Theta + 2\pi\hbar > 0$ the spectrum is continuous, while for $\Theta + n2\pi\hbar < 0$ we find discrete values E_k [15]

$$\Theta + n2\pi\hbar = E_k = -\tfrac{1}{8}\hbar^2\left(-(1+2k) + \sqrt{1+\tfrac{8\lambda}{\hbar^2}}\right)^2. \quad (31)$$

The "diagonal" Hamiltonian is a direct sum of these particular equations over all n. Similarly its spectrum is nothing but the sum of the particular spectra and consists of a continuous part (the whole real axis) with embedded eigenvalues.

As we have seen from our numerical calculations, states belonging to different channels n are only slightly mixed up by the scattering process for small λ. In this case we can take the nondiagonal part of Eq. (29) as a perturbation to the diagonal part.

The embedded eigenvalues are highly unstable and disappear as soon as the perturbation is switched on. Howland [16,17] has demonstrated that the eigenvalues that

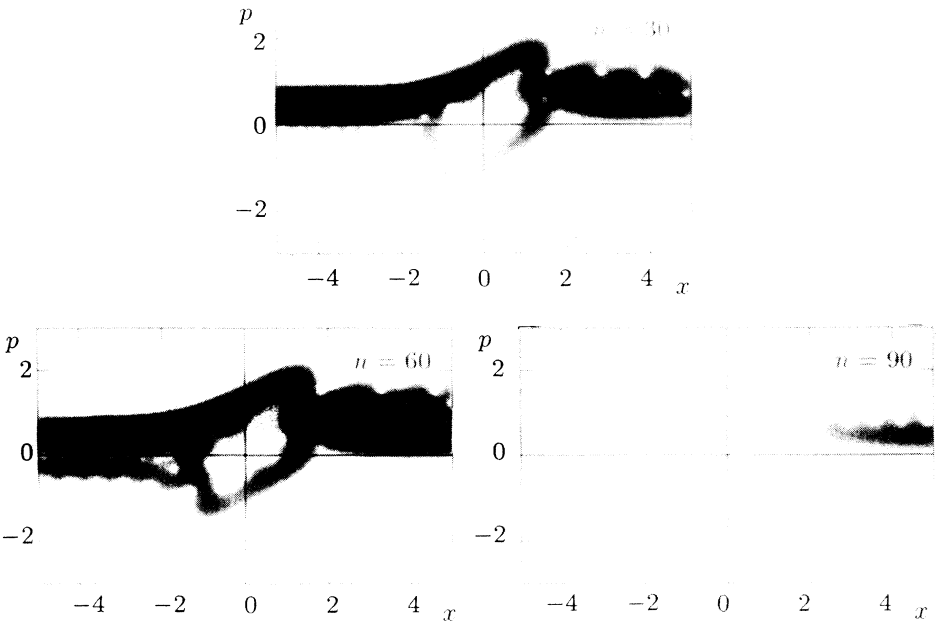

FIG. 10. The Husimi function of a scattered quantum particle which is out of the resonance. Only small parts of the wave function enter the orbit around the classical stability island.

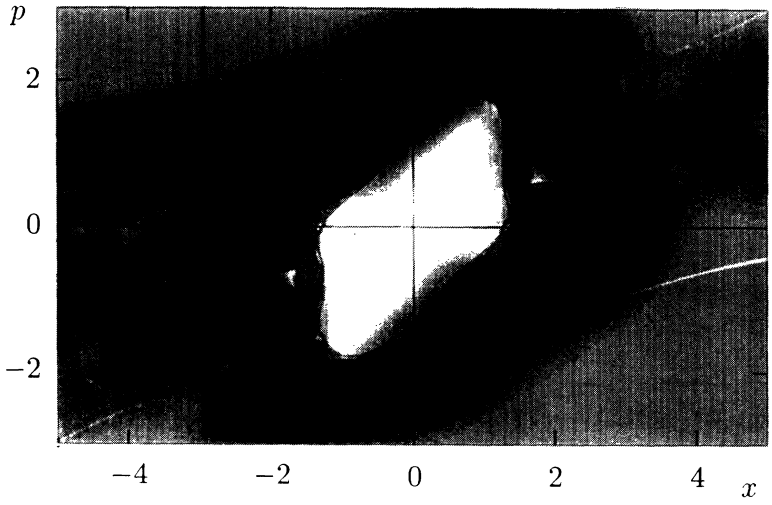

FIG. 11. The orbit at the border of the stability island. Parts of the Husimi function stick into the classical stability island. The integral of the Husimi function over the stability island is taken to define the "tunneling rate" $I(\theta)$.

have "disappeared" become complex poles of the S matrix (resonances). For small λ these poles are close to the real axis and can be observed as sharp maxima of the corresponding reflection coefficients which are localized in the neighborhood of the embedded eigenvalues of the "diagonal" part of Eq. (29). Our numerical calculations (see Fig. 8) show that the maxima of the reflection coefficients really stay in the neighborhood of the shifted eigenvalues E_k, when we vary the coupling constant λ. For large λ, the nondiagonal part of Eq. (29) becomes more important; the resonances leave the real axis and superpose to Ericson fluctuations.

IV. QUANTUM DESCRIPTION IN PHASE SPACE

In this section we would like to connect the observed quantum resonances with a tunneling into the classical stability island. The correspondence between the quantum wave function and the classical phase space is described by the Husimi function $\rho_H(x,p)$ [18]:

$$\rho_H(x,p) = (2\pi\hbar)^{-1}|\langle\varphi_{xp}|\psi\rangle|^2, \tag{32}$$

with

$$\langle x'|\varphi_{xp}\rangle = \left(2\pi\Delta x^2\right)^{-1/4}\exp\left(\tfrac{i}{\hbar}px' - \frac{(x'-x)^2}{2\Delta x^2}\right),$$

$$\Delta x = \sqrt{\hbar/2}. \tag{33}$$

Observing the way the quantum particle travels through the phase space by computing its Husimi function we see that in the cases with resonant reflection the wave function enters an orbit around the stability island where it stays for a long time (see Fig. 9). Outside the resonance, only small parts of the wave function enter the orbit (see Fig. 10).

As one can see in Fig. 11, parts of the Husimi function are even located inside the stability island so we can speak about "tunneling" of the quantum particle into the stability island. For a quantitative check we introduce the *tunneling rate* I as the integral of the Husimi function over the classical stability island $\mathcal{I}$:

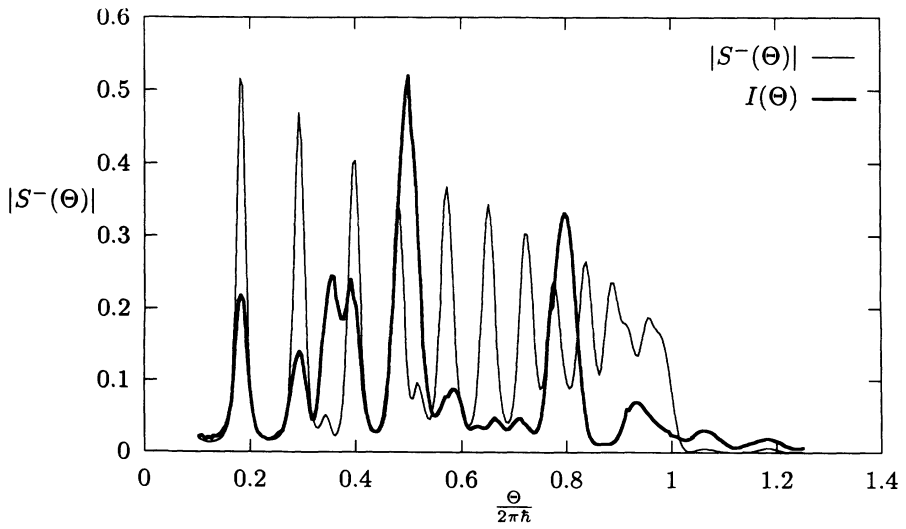

FIG. 12. The reflection coefficient $S^-(\Theta)$ and the tunneling rate $I(\Theta)$. The maxima are located at the same places, but the very small maxima of $S^-(\Theta)$ [belonging to $n = 2$ in Eq. (31)] are emphasized in $I(\Theta)$. For smaller λ, both curves become more similar (not shown).

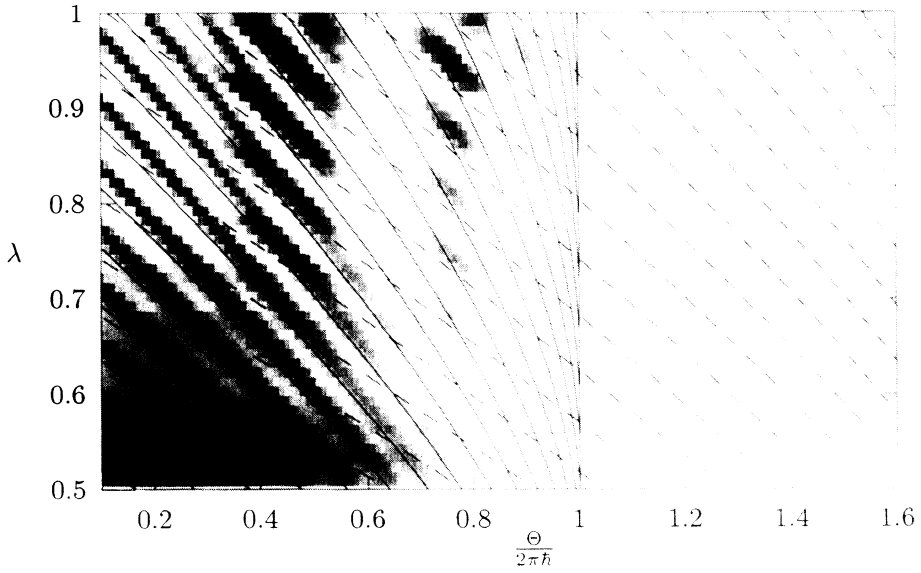

FIG. 13. Gray scale plot of the tunneling rate I as a function of Θ and λ. The picture is close to that of the reflection coefficient $S^-(\Theta)$ (Fig. 8), but maxima belonging to $n = 2$ are emphasized, so the highest maxima are lying near the crossing points of the lines of the shifted eigenvalues for $n = 1$ and $n = 2$.

$$I := \iint_{\mathcal{I}} dx\, dp\, \rho_H(x,p). \tag{34}$$

When we compute I for different Θ and compare it with the total reflection coefficient $S^-(\Theta)$ [the sum of $S^-_{n,n'}(\Theta)$ for fixed Θ and n' over all n—see Fig. 12], we see that the maxima of both curves are located at the same places. The heights of the maxima are different: The very small maxima of S^-, which belong to $n = 2$ [n as in Eq. (31)], are much bigger for $I(\Theta)$. When we change λ we get similar pictures (see Figs. 13 and 8), but we notice the largest values for $I(\Theta)$ in the neighborhood of the crossing points between the lines of the shifted eigenvalues for $n = 1$ and $n = 2$ in Eq. (20).

ACKNOWLEDGEMENT

This work was supported by the Sonderforschungsbereich 237 *Unordnung und große Fluktuationen* of the Deutsche Forschungsgemeinschaft.

[1] B. Eckhardt and C. Jung, J. Phys. A: Math. Gen. **19**, L829 (1986).
[2] T. Tel, J. Phys. A **22**, L691 (1989).
[3] S. Bleher, E. Ott, and C. Grebogi, Phys. Rev. Lett. **63**, 919 (1989).
[4] R. Blümel and U. Smilansky, Phys. Rev. Lett. **60**, 477 (1988).
[5] P. Gaspard and S. A. Rice, J. Chem. Phys. **90**, 2242 (1989).
[6] P. Gaspard and S. A. Rice, J. Chem. Phys. **90**, 2255 (1989).
[7] P. Brumer and M. Shapiro, Adv. Chem. Phys. **70**, 365 (1988).
[8] C. Jung and T. Tel, J. Phys. A: Math. Gen. **24**, 2793 (1991).
[9] C. F. F. Karney, Physica **8D**, 360 (1983).
[10] J. D. Meis and E. Ott, Phys. Rev. Lett. **55**, 2741 (1985).
[11] R. S. Dumont and P. Brumer, Chem. Phys. Lett. **188**, 565 (1992).
[12] Y.-C. Lai, R. Blümel, E. Ott, and C. Grebogi, Phys. Rev. Lett. **68**, 3491 (1992).
[13] K. Yajima, J. Math. Soc. Jpn. **29**, 729 (1977).
[14] J. S. Howland, Ind. Univ. Math. J. **28**, 471 (1979).
[15] L. D. Landau and E. M. Lifschitz, *Kvantovaya Mekhanika (nerelativistskaya teoriya)* (Nauka, Moscow, 1974), Sec. 23.
[16] J. S. Howland, Bull. Am. Math. Soc. **78**, 280 (1972).
[17] J. S. Howland, Pacific J. Math. **55**, 157 (1974).
[18] K. Takahashi, Prog. Theor. Phys. Supp. **98**, 109 (1989).

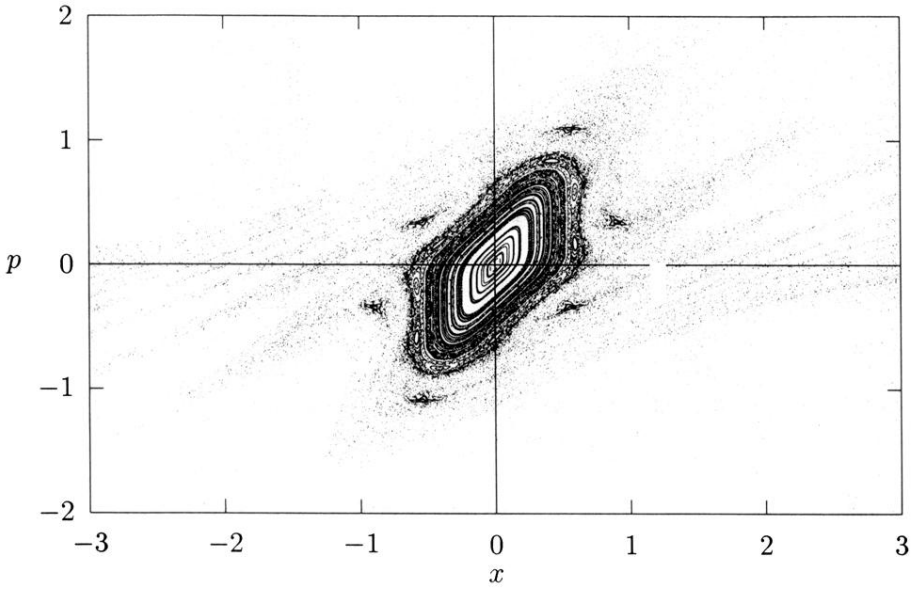

FIG. 1. Poincaré plot for $\lambda = 1$. In the center we see a large "stability island" which is embedded in a chaotic layer.

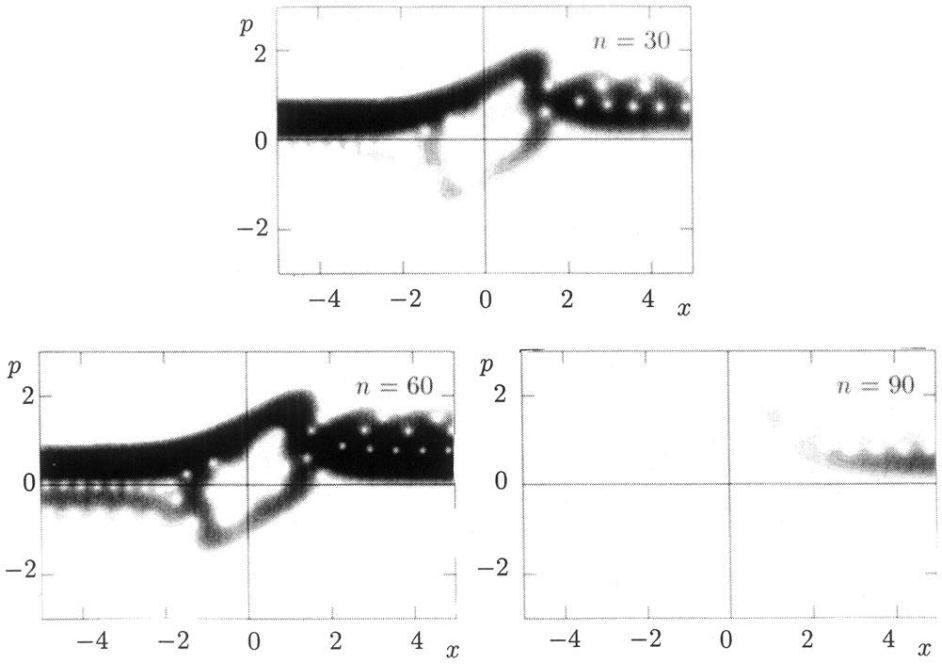

FIG. 10. The Husimi function of a scattered quantum particle which is out of the resonance. Only small parts of the wave function enter the orbit around the classical stability island.

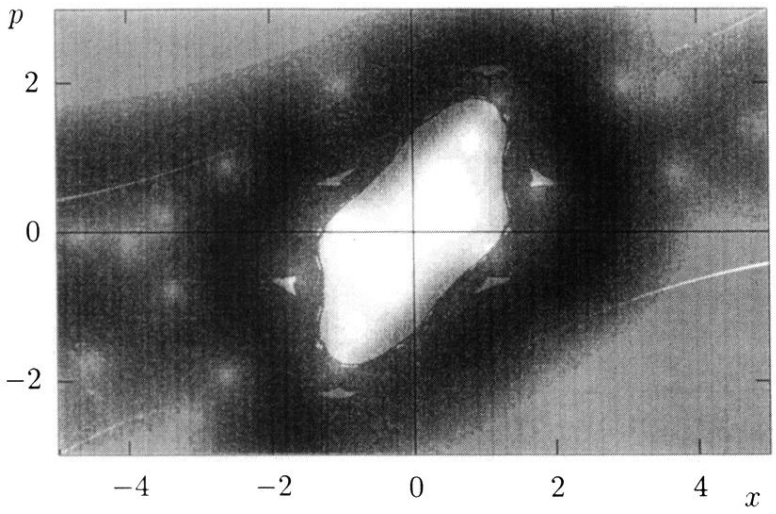

FIG. 11. The orbit at the border of the stability island. Parts of the Husimi function stick into the classical stability island. The integral of the Husimi function over the stability island is taken to define the "tunneling rate" $I(\theta)$.

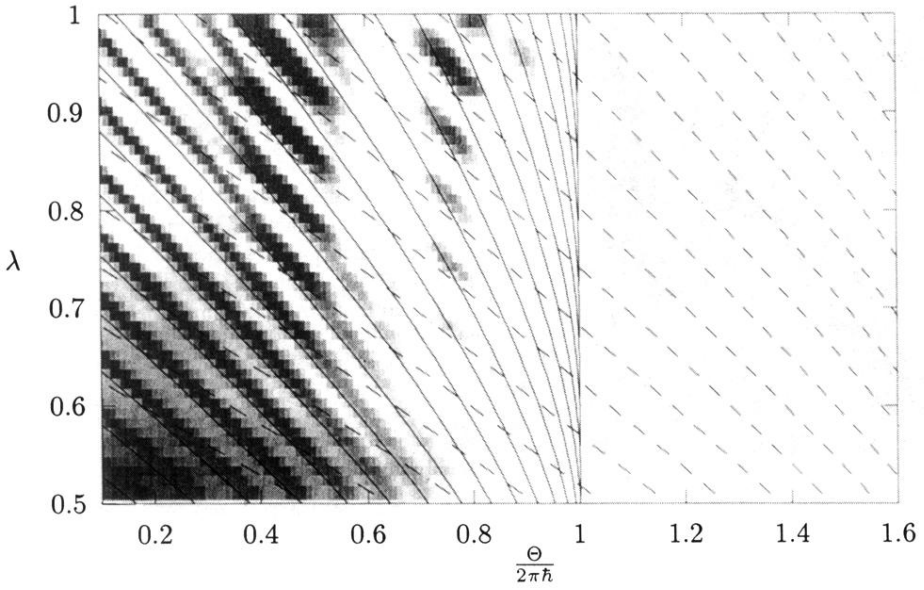

FIG. 13. Gray scale plot of the tunneling rate I as a function of Θ and λ. The picture is close to that of the reflection coefficient $S^{-}(\Theta)$ (Fig. 8), but maxima belonging to $n = 2$ are emphasized, so the highest maxima are lying near the crossing points of the lines of the shifted eigenvalues for $n = 1$ and $n = 2$.

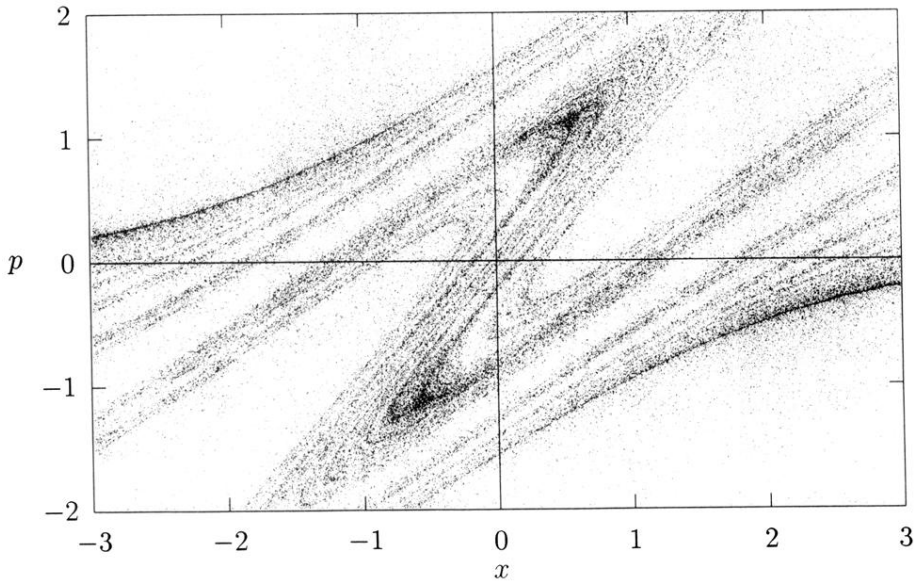

FIG. 2. Poincaré plot for $\lambda = 3$. The phase space is dominated by chaos.

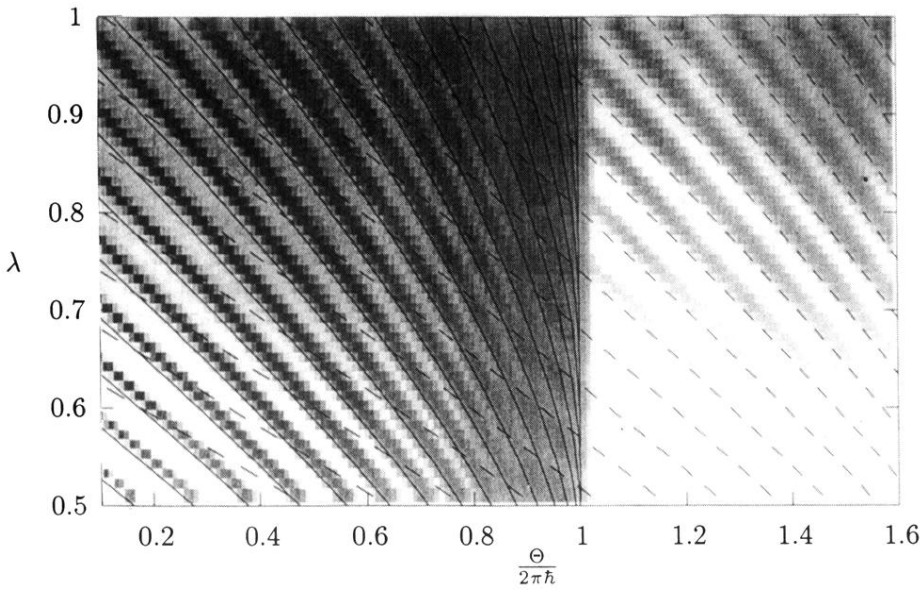

FIG. 8. Gray scale plot of the total reflection coefficient $S^{-}(\Theta)$ as a function of Θ and λ. The solid lines stand for eigenvalues E_k of a corresponding time-independent system, shifted by $2\pi\hbar$; the dashed lines denote $E_k + 2 \times 2\pi\hbar$.

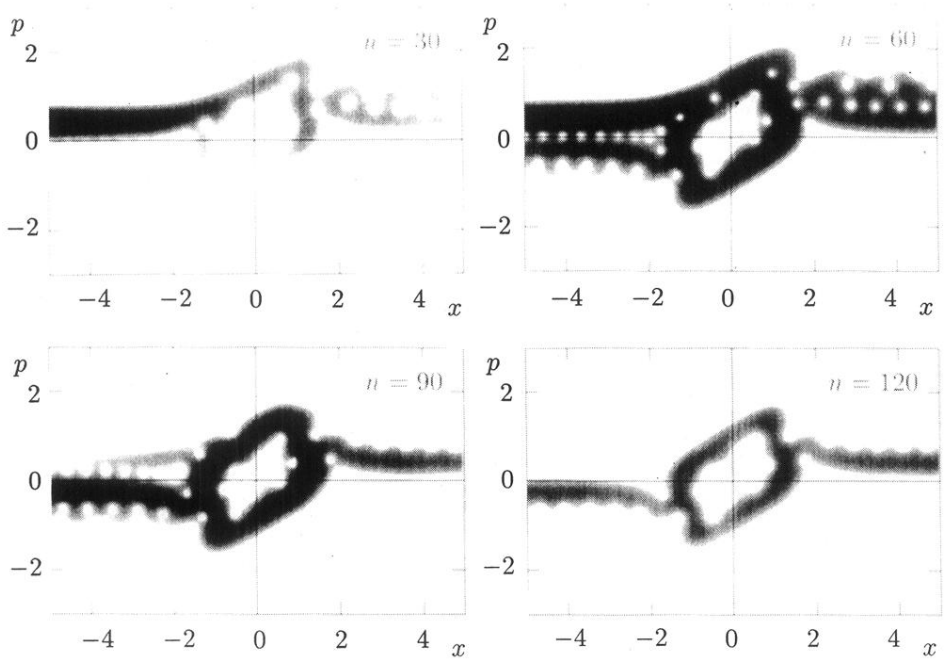

FIG. 9. The Husimi function of a scattered quantum particle with maximum reflection coefficient. The wave function enters a quasistable orbit at the border of the classical stability island.